

MCTDHF in Ultrafast Laser Dynamics

Othmar Koch
Wolfgang Kreuzer
Armin Scrinzi

AURORA TR2003-29

Institute for Applied Mathematics and Numerical Analysis
Vienna University of Technology
Wiedner Hauptstrasse 8-10, A-1040 Wien, Austria

E-Mail: othmar@fsmat.at
kreuzer@aurora.anum.tuwien.ac.at

The work described in this report was supported by the Special Research Program SFB F011
“AURORA” of the Austrian Science Fund FWF.

Introduction

This report describes an approach to the numerical solution of the time-dependent Schrödinger equation arising in ultrafast laser dynamics.

Large-scale computations of electronic structure and dynamics pose extremely challenging problems in several areas of research.

For static electronic structure computations, many different methods have been developed in various fields, such as theoretical physics or theoretical and computational chemistry. To improve on the solution of the time-independent Schrödinger equation by direct discretization, methods like *density functional theory (DFT)* or (*multiconfiguration Hartree-Fock (MCHF)*) have been suggested.

DFT is a powerful method to reduce the Schrödinger equation for f degrees of freedom from a linear problem in \mathbb{R}^{3f} to a set of f nonlinear equations in \mathbb{R}^3 , where the computational effort scales with the degrees of freedom as f^2 . DFT has found its most prominent applications in the calculation of ground-state properties of systems with many particles such as solids. MCHF, in turn, is one of the most powerful standard tools in electronic structure calculations of atoms and small molecules. Similar to DFT, MCHF reduces the Schrödinger equation to a coupled set of nonlinear equations, but with much less favorable scaling behavior of the order n^4 where $n \geq f$. For few particle systems, this entails a tolerable increase of computational effort. In contrast to DFT, increasing n allows to, in principle, systematically improve the approximation of the original Schrödinger equation by MCHF. In both, DFT and MCHF, (nonlinear) eigenvalue problems have to be solved.

Ultrashort strong laser pulses, however, require the solution of time-dependent, initial value problems. These laser pulses developed during the last few years have opened a new regime in the interaction of fields with matter [13]. One of the most intriguing aspects is the possibility of ultrashort time-resolved spectroscopy in the sub-femtosecond time domain. The present state of the art of numerically solving the time-dependent Schrödinger equation directly for realistic laser pulses is limited to two electron systems. The most successful calculations involve the largest massively parallel computers available [1], [17]. It is clear that the direct solution of the linear time-dependent Schrödinger equation has reached its computational limits.

The use of density functional theory for this problem is limited at least by two problems: The known approximations of the crucial “exchange correlation” term, while producing consistent ground state energies, generate contradictory and incorrect dynamical behavior [21] and there is no applicable theory for the description of multi-electron processes, such as detachment of two electrons from an atom. While this approach promises an enormous reduction in the complexity of the computational problems, the theory is not yet developed far enough so as to be applicable to our problem.

Therefore our method of choice to make the original, linear Schrödinger equation tractable for numerical computation, is the multiconfiguration time-dependent Hartree-Fock method (MCTDHF) [22], [24]. This approach produces a lower-dimensional, nonlinear system of coupled Schrödinger equations, which is solved, for instance, by the

method of lines. Initially, simple finite differences are chosen for space discretization, an approach which may be inferior to pseudospectral methods (Fourier collocation) [12]. For time integration, splitting methods similar to those proposed and analyzed for MCTDH [16] are applied.

Chapter 1

The Model

We are interested in the solution of the time-dependent Schrödinger equation for an atom or molecule with f degrees of freedom in a time-dependent electric field (typically arising from ultrashort laser pulses),

$$i \frac{\partial \psi}{\partial t} = H \psi, \quad (1.1)$$

where the complex-valued *wave function* $\psi = \psi(x_1, \dots, x_f, t)$ explicitly depends on time t and, in the case considered here, the positions x_1, \dots, x_f of electrons in an atom or molecule. The Hamiltonian H is time-dependent and has the form

$$H := \sum_{k=1}^f \left(\frac{1}{2} (-i \nabla_k - A(t))^2 + U(x_k) + \sum_{l \neq k} V(x_k - x_l) \right), \quad (1.2)$$

where

$$U(x) := - \sum_{l=1}^f \frac{1}{\sqrt{a^2 + (x - 1.4l)^2}}, \quad (1.3)$$

$$V(x - y) := \frac{1}{\sqrt{1 + (x - y)^2}}, \quad (1.4)$$

$$A(t) := e^{-(t/\tau)^2} \sin(\omega t) A_0. \quad (1.5)$$

∇_k is the nabla operator w. r. t. x_k only. For this potential, the internuclear distance is fixed at 1.4, and for each molecule the screening parameter a is adjusted such that the ionization potential is 0.3 independent of f [22], [24]. Moreover, ω is of order of magnitude 10^{-1} , $\tau = \frac{2\pi}{\omega} n$, where $n \in \mathbb{R}$ is of order of magnitude 10, and A_0 is a constant, $A_0 = O(1)$. For the moment, we restrict ourselves to problems in one space dimension.

1.1 The MCTDHF Approach

In [22], [24], a new approach for the approximate solution of the time-dependent Schrödinger equation was introduced: The multi-electron wave function ψ from

(1.1) is approximated by a function satisfying the ansatz

$$\begin{aligned}\psi(x_1, \dots, x_f, t) &= \sum_{(j_1, \dots, j_f)} a_{j_1, \dots, j_f}(t) \phi_{j_1}(x_1, t) \cdots \phi_{j_f}(x_f, t) \\ &=: \sum_J a_J \Phi_J(x, t).\end{aligned}\quad (1.6)$$

In (1.6), we are only interested in solutions ψ which are antisymmetric under exchange of any two of their arguments x_j, x_k . This assumption is particular to the MCTDHF approach, as compared to MCTDH considered, for example, in [2], [3] or [16], and reduces the number of equations considerably. Particularly, the assumption implies antisymmetry in the coefficients a_J . Formally, multiindices $J = (j_1, \dots, j_f)$ vary for $j_k = 1, \dots, N, k = 1, \dots, f$. Due to the simplifications resulting from the symmetry assumption, only $\binom{N}{f}$ equations for a_J have to be solved in the actual computations, however. Nonetheless, we keep this description close to [2] for convenience of notation.

We use the Frenkel-Dirac variational principle [5], [8] to derive differential equations for the coefficients a_J and the *single-particle functions* ϕ_k . Thus, we require that for ψ in the manifold \mathcal{M} of functions of the form of the ansatz (1.6),

$$\left\langle \delta\psi \left| i \frac{\partial}{\partial t} - H \right| \psi \right\rangle = 0, \quad (1.7)$$

where $\delta\psi$ varies in the tangent space $\mathcal{T}_\psi \mathcal{M}$ of \mathcal{M} at ψ , i. e.,

$$\mathcal{T}_\psi \mathcal{M} = \left\{ \delta\psi : \delta\psi(x, t) = \sum_J \left(\delta a_J \Phi_J(x, t) + a_J \sum_{k=1}^f \delta\phi_{j_k}(x_k) \prod_{l \neq k} \phi_{j_l}(x_l) \right) \right\},$$

where $\delta a_J \in \mathbb{C}$ and $\delta\phi_{j_k} \in L^2$.

In order to define a unique solution of (1.7), we impose additional constraints,

$$\langle \phi_j | \phi_k \rangle = \delta_{j,k}, \quad t = 0, \quad (1.8)$$

$$\left\langle \phi_j \left| \frac{\partial \phi_k}{\partial t} \right. \right\rangle = -i \langle \phi_j | g | \phi_k \rangle, \quad t \geq 0, \quad (1.9)$$

where we have the freedom of choice to use any Hermitian operator g . Usually, we set $g \equiv 0$ for reasons of simplicity. In the context of the variational splitting described in [16], we will discuss the role of nontrivial g , however. (1.8) together with (1.9) guarantees that the relation from (1.8) holds for all $t \geq 0$. This is the subject of the following lemma.

Lemma 1.1.1 *Assume that (1.8) and (1.9) hold. Then*

$$\langle \phi_j | \phi_k \rangle = \delta_{j,k}, \quad t \geq 0. \quad (1.10)$$

Proof: Obviously, it is sufficient to show

$$\frac{d}{dt} \langle \phi_j | \phi_k \rangle = 0.$$

This relation can easily be proven using (1.9) and taking into account the fact that g is Hermitian operator:

$$\begin{aligned} \frac{d}{dt} \langle \phi_j | \phi_k \rangle &= \left\langle \phi_j \left| \frac{\partial \phi_k}{\partial t} \right. \right\rangle + \left\langle \frac{\partial \phi_j}{\partial t} \left| \phi_k \right. \right\rangle \\ &= \left\langle \phi_j \left| \frac{\partial \phi_k}{\partial t} \right. \right\rangle + \overline{\left\langle \phi_k \left| \frac{\partial \phi_j}{\partial t} \right. \right\rangle} \\ &= -i \langle \phi_j | g | \phi_k \rangle + i \overline{\langle \phi_k | g | \phi_j \rangle} \\ &= -i \langle \phi_j | g | \phi_k \rangle + i \langle \phi_j | g | \phi_k \rangle \\ &= 0. \end{aligned}$$

□

The variational principle (1.7) and the additional restrictions (1.9) and (1.9), finally yield the “working equations”

$$i \frac{da}{dt} = A_H(\phi)a, \quad (1.11)$$

$$i \frac{\partial \phi}{\partial t} = B_H(a, \phi)\phi, \quad (1.12)$$

for $a = (a_{j_1, \dots, j_f})$, $\phi = (\phi_k)$. In equation (1.11),

$$[A_H(\phi)]_{J,L} := \langle \Phi_J | H | \Phi_L \rangle \quad (1.13)$$

is a “Galerkin matrix”, and (1.12) is derived from

$$i \rho \frac{\partial \phi}{\partial t} = (I - P) \bar{H} \phi, \quad (1.14)$$

where

$$\psi_j := \langle \phi_j | \psi \rangle, \quad (\text{“single-hole functions”}), \quad (1.15)$$

$$\rho_{j,l} := \langle \psi_j | \psi_l \rangle, \quad (\text{“density matrix”}), \quad (1.16)$$

$$\bar{H}_{j,l} := \langle \psi_j | H | \psi_l \rangle, \quad (\text{“mean field operator matrix”}), \quad (1.17)$$

and P is the orthogonal projector onto the space spanned by the functions ϕ_k . In (1.15), the L^2 scalar product is defined with respect to the argument of ϕ_j only, while in (1.16) the integration is defined over all variables except one, and the mean-field operator matrix from (1.17) contains operators acting on one spatial variable, say x_k .

Note that the equivalence of (1.12) and (1.14) is not trivial and requires some further discussion. In cases where the density matrix ρ is singular¹, a special treatment is necessary. In this case, a careful analysis of the conditioning of the resulting least squares problem is required. We discuss the numerical implications in Section 2.2.3.

1.2 A Simple Example

In this section, we derive a simple example, where the working equations (1.11) and (1.12) can be stated explicitly. To illustrate the approach outlined in Section 1.1, we apply the variational principle (1.7), and compare the resulting equations with (1.11) and (1.12) derived as in [2]. The test example we consider here describes the non-restricted two-particle single-configuration Hartree-Fock method, where $N = f = 2$. This situation might, for instance, arise in computations for the Helium atom.

For concise notation, we write

$$\phi_{ik} := \phi_i(x_k, t). \quad (1.18)$$

The only *Hartree-products* Φ_J present in our computations are

$$\Phi_{12} = \phi_{11}\phi_{22}, \quad \Phi_{21} = \phi_{21}\phi_{12}. \quad (1.19)$$

The ansatz (1.6) thus becomes

$$\Psi := a_{12}(\Phi_{12} - \Phi_{21}).$$

Note that the additional constraints (1.8) and (1.9) imply

$$\langle \Phi_L | \Phi_K \rangle = \delta_{LK}, \quad \langle \Phi_L | \dot{\Phi}_K \rangle = 0. \quad (1.20)$$

To derive an equation for a_{12} directly from the variational principle, we vary a_{12} and make use of the antisymmetry inherent in the MCTDHF approach, which implies the relation

$$\left\langle \Phi_{12} - \Phi_{21} \left| H - i \frac{\partial}{\partial t} \right| a_{12}(\Phi_{12} - \Phi_{21}) \right\rangle = 0. \quad (1.21)$$

Rewriting (1.21) we obtain (cf. (1.20))

$$a_{12} \langle \Phi_{12} - \Phi_{21} | H | \Phi_{12} - \Phi_{21} \rangle - i \dot{a}_{12} \langle \Phi_{12} - \Phi_{21} | \Phi_{12} - \Phi_{21} \rangle - \quad (1.22)$$

$$-i a_{12} \langle \Phi_{12} - \Phi_{21} | \dot{\Phi}_{12} - \dot{\Phi}_{21} \rangle = \quad (1.23)$$

$$a_{12} \langle \Phi_{12} - \Phi_{21} | H | \Phi_{12} - \Phi_{21} \rangle - 2i \dot{a}_{12} = 0. \quad (1.24)$$

¹This may occur for example when one of the single particle functions ϕ_j does not appear in the expansion (1.6), i. e., $a_j = 0$ whenever j occurs in J .

Further calculations (which we do not report here) using the antisymmetry under exchange of any two electrons (which is inherent in the MCTDHF ansatz, but *not* in the original MCTDH equations), finally yield

$$i\dot{a}_{12} = a_{12}\langle\Phi_{12}|H|\Phi_{21} - \Phi_{12}\rangle. \quad (1.25)$$

If alternatively we use equation (1.13) without taking into account the antisymmetry in the coefficients, we obtain equations for both a_{12} and a_{21} ,

$$i\dot{a}_{12} = \langle\Phi_{12}|H|\Phi_{12}\rangle a_{12} + \langle\Phi_{12}|H|\Phi_{21}\rangle a_{21} \quad (1.26)$$

$$= a_{12}\langle\Phi_{12}|H|\Phi_{12} - \Phi_{21}\rangle, \quad (1.27)$$

and

$$i\dot{a}_{21} = a_{12}\langle\Phi_{21}|H|\Phi_{12} - \Phi_{21}\rangle. \quad (1.28)$$

Combining these equations and using $a_{12} = -a_{21}$, we again obtain (1.24).

To compute an equation for ϕ_{11} directly from the variational principle, we now vary ϕ_{11} . Rewriting the resulting equation

$$\left\langle a_{12}\phi_{22} \left| H - i\frac{\partial}{\partial t} \right| a_{12}(\Phi_{12} - \Phi_{21}) \right\rangle = 0, \quad (1.29)$$

we obtain

$$|a_{12}|^2\langle\phi_{22}|H|\Phi_{12} - \Phi_{21}\rangle - ia_{12}^*\dot{a}_{12}\langle\phi_{22}|\phi_{11}\phi_{22} - \phi_{21}\phi_{12}\rangle \quad (1.30)$$

$$-i|a_{12}|^2\langle\phi_{22}|\dot{\phi}_{11}\phi_{22} + \phi_{11}\dot{\phi}_{22} - \dot{\phi}_{21}\phi_{12} - \phi_{21}\dot{\phi}_{12}\rangle = 0. \quad (1.31)$$

Finally, using (1.24) and (1.20) this results in the equation

$$i\dot{\phi}_{11} = \langle\phi_{22}|H|\Phi_{12} - \Phi_{21}\rangle - \frac{1}{2}\langle\Phi_{12} - \Phi_{21}|H|\Phi_{12} - \Phi_{21}\rangle\phi_{11}. \quad (1.32)$$

Alternatively we use (1.14), where in our special case the single-hole functions are defined as

$$\begin{aligned} \psi_{11} &:= a_{12}\phi_{22}, & \psi_{12} &:= -a_{12}\phi_{21} \\ \psi_{21} &:= -a_{12}\phi_{12}, & \psi_{22} &:= a_{12}\phi_{11}. \end{aligned}$$

Using the constraints (1.8) and (1.9) in the computation of ρ , we obtain $\rho = |a_{12}|^2\text{diag}(1, 1)$. The resulting equation for $\dot{\phi}_{11}$ is

$$i\dot{\phi}_{11} = (1 - P)(\langle\phi_{22}|H|\phi_{22}\rangle\phi_{11} - \langle\phi_{22}|H|\phi_{12}\rangle\phi_{21}).$$

This is equivalent to

$$i\dot{\phi}_{11} = \langle \phi_{22} | H | \phi_{22} \rangle \phi_{11} - \langle \phi_{22} | H | \phi_{12} \rangle \phi_{21} - \quad (1.33)$$

$$- \langle \phi_{11} \phi_{22} | H | \phi_{11} \phi_{22} \rangle \phi_{11} + \langle \phi_{11} \phi_{22} | H | \phi_{12} \phi_{21} \rangle \phi_{11} - \quad (1.34)$$

$$- \langle \phi_{21} \phi_{22} | H | \phi_{11} \phi_{22} \rangle \phi_{21} + \langle \phi_{21} \phi_{22} | H | \phi_{12} \phi_{21} \rangle \phi_{21} \quad (1.35)$$

$$= \langle \phi_{22} | H | \Phi_{12} - \Phi_{21} \rangle - \langle \Phi_{12} | H | \Phi_{12} - \Phi_{21} \rangle \phi_{11} - \quad (1.36)$$

$$- \langle \phi_{21} \phi_{22} | H | \Phi_{21} - \Phi_{12} \rangle \phi_{21}. \quad (1.37)$$

Equations (1.32) and (1.37) differ in the term

$$- \langle \phi_{21} \phi_{22} | H | \Phi_{21} - \Phi_{12} \rangle \phi_{21}. \quad (1.38)$$

This expression is equal to 0, however. This can easily be seen from substitution of $\Phi_{22} := \phi_{21} \phi_{22}$ into [2, (31)], which reads

$$\langle \Phi_J | H | \Psi \rangle = i \langle \Phi_J | \dot{\Psi} \rangle. \quad (1.39)$$

Consequently,

$$\langle \Phi_{22} | H | \Psi \rangle = i \dot{a}_{12} \langle \Phi_{22} | \Phi_{12} - \Phi_{21} \rangle - i a_{12} \langle \Phi_{22} | \dot{\Phi}_{12} - \dot{\Phi}_{21} \rangle = 0, \quad (1.40)$$

and we conclude

$$\langle \Phi_{22} | H | \Phi_{21} - \Phi_{12} \rangle = 0.$$

This reflects the antisymmetry in the ansatz (1.6).

Analogously, we can also derive a differential equation for ϕ_{21} , either directly using the variational principle or from (1.14). Again, the same expression results from both calculations. In summary, the working equations for the test example with $N = f = 2$ read

$$\begin{aligned} i\dot{a}_{12} &= \langle \phi_1(x_1) \phi_2(x_2) | H | \phi_1(x_1) \phi_2(x_2) - \phi_2(x_1) \phi_1(x_2) \rangle a_{12} \\ &= \langle \Phi_{12} | H | \Phi_{12} - \Phi_{21} \rangle a_{12} \end{aligned} \quad (1.41)$$

$$i\dot{\phi}_i(x) = (1 - P) \sum_{k=1}^2 \langle \tilde{H} \rangle_{ik} \phi_k(x) \quad i = 1, 2, \quad (1.42)$$

where

$$P = |\phi_1\rangle \langle \phi_1| + |\phi_2\rangle \langle \phi_2| \quad (1.43)$$

and

$$\langle \tilde{H} \rangle_{11} = \langle \phi_2 | H | \phi_2 \rangle, \quad (1.44)$$

$$\langle \tilde{H} \rangle_{22} = \langle \phi_1 | H | \phi_1 \rangle, \quad (1.45)$$

$$\langle \tilde{H} \rangle_{12} = - \langle \phi_2 | H | \phi_1 \rangle, \quad (1.46)$$

$$\langle \tilde{H} \rangle_{21} = - \langle \phi_1 | H | \phi_2 \rangle. \quad (1.47)$$

Chapter 2

Solution Techniques

2.1 Variational Splitting

It has been suggested in [16] for a Hamiltonian $H = T + V$ to use splitting methods to separate the computations for the “kinetic part”

$$T := - \sum_{k=1}^f \frac{1}{2} \Delta_k$$

and the “potential energy operator” $V := V(x_1, \dots, x_f)$. The advantage is apparent if we note that a space discretization with mesh width Δx implies that the time integration suffers from severe restrictions on Δt in relation to Δx . If the discretized Laplacian $T_{\Delta x}$ is treated in a separate time step, this step size restriction does not apply in the computations for V .

Unfortunately, splitting methods cannot be applied in the usual way in the solution of (1.11) and (1.12), because the coupling of T and V is too intricate in this formulation. Consequently, splitting is used at the level of the variational equations (1.7).

In our case, we use splitting of the Hamiltonian $H := T + V$ from (1.2) into the parts

$$T := \sum_{k=1}^f \left(\frac{1}{2} (-i\nabla_k - A(t))^2 + U(x_k) \right), \quad (2.1)$$

$$V := \sum_{k=1}^f \sum_{l \neq k} V(x_k - x_l), \quad (2.2)$$

where T is the single-particle part which consists of operators acting on only one particle at a time, and V describes particle-particle interactions.

Thus, one step of the variational splitting method starting at $t = t_0$ with time step Δt is defined as follows:

1. Compute $\psi_{1/2}^- \in \mathcal{M}$ as the solution at time $t_0 + \frac{1}{2}\Delta t$ of

$$\left\langle \delta\psi \left| i \frac{\partial}{\partial t} - T \right| \psi \right\rangle = 0 \quad \forall \delta\psi \in \mathcal{T}_\psi \mathcal{M}, \quad (2.3)$$

with initial value $\psi(t_0) = \psi_0$.

2. Compute $\psi_{1/2}^+ \in \mathcal{M}$ as the solution at time $t_0 + \Delta t$ of

$$\left\langle \delta\psi \left| i\frac{\partial}{\partial t} - V \right| \psi \right\rangle = 0 \quad \forall \delta\psi \in \mathcal{T}_\psi \mathcal{M}, \quad (2.4)$$

with initial value $\psi(t_0) = \psi_{1/2}^-$.

3. Compute $\psi_1 \in \mathcal{M}$ as the solution at time $t_0 + \Delta t$ of (2.3) with initial value $\psi(t_0 + 1/2\Delta t) = \psi_{1/2}^+$.

Now, since $T\psi \in \mathcal{T}_\psi \mathcal{M}$ for $\psi \in \mathcal{M} \cap H^2$, the two steps of the form (2.3) are equivalent to solving the Schrödinger equations

$$i\frac{\partial\psi}{\partial t} = T\psi \quad (2.5)$$

on the respective domains. If the initial function is chosen in \mathcal{M} , (2.5) decouples into a set of single particle Schrödinger equations:

$$\frac{da_J}{dt} = 0, \quad \forall J, \quad (2.6)$$

$$i\frac{\partial\phi_j}{\partial t} = \frac{1}{2}(-i\nabla - A(t))^2 \phi_j + U\phi_j, \quad j = 1, \dots, N. \quad (2.7)$$

It depends on the space discretization of the Laplacian how these equations can be solved most efficiently. As a first try, simple (symmetric) finite differences have been implemented, and (2.7) was solved using the box scheme for time discretization (in physics, this discretization method is often denoted as *Crank-Nicholson method*). The different approaches are discussed in Section 2.2.2.

The second splitting step (2.4) leads to equations

$$i\frac{da}{dt} = A_V(\phi)a, \quad (2.8)$$

$$i\frac{\partial\phi}{\partial t} = B_V(a, \phi)\phi. \quad (2.9)$$

where A_V and B_V are defined analogously as in (1.11) and (1.12), using the operator V instead of H .

Remark: An alternative interpretation of the variational splitting approach follows from observations in [2]. If we choose g in the general constraint (1.9) as the part of H which acts only on one degree of freedom,

$$g := T,$$

a partially separated form of the working equations arises, see [2, (43),(44)]. If splitting is applied to these equations, this results in the equations (2.6) and

(2.7) for the single particle parts and (2.8) and (2.9) for the residual part of the Hamiltonian. Consequently, variational splitting is equivalent to splitting of the working equations, if a special constraint (1.9) is imposed. Eq. (1.10) is not affected by these considerations, this important relation follows even when the Hermitian operator g depends on t .

2.2 Numerical Realization

2.2.1 The Original MCTDHF Code

In the original MCTDHF code [22], [24], no splitting methods are employed to separate strongly varying from smooth modes. Rather, (1.11) and (1.12) are solved directly. For space discretization, second order finite differences at equidistant points are used.

The resulting ODEs in time are solved using a variable order, variable step size explicit Runge-Kutta method. For error estimation in the time integration, extrapolation based on mesh halving is used.

Relation (1.10) is explicitly enforced after every Runge-Kutta step using the Gram-Schmidt method.

The Constant Mean-Field (CMF) Integration Method

Let us briefly mention the integration scheme proposed in [2] and [3] for the numerical solution of the (full) working equations (1.11) and (1.12). The main idea is to use a splitting-type approach which takes into account the fact that for problems considered for solution with MCTDH, the variation in the single particle functions ϕ_j and coefficients a_j is much faster than the variation in the density matrix ρ and the mean-field operator matrix \bar{H} . The evaluation of the two latter quantities is computationally very expensive due to the nonlocal nature of the quantities and the resulting high-dimensional numerical quadrature at a vast number of nodes, see Section 2.2.3. Moreover, since symmetry cannot be used in MCTDH, the system (1.11) has very high dimension. Consequently, it seems favorable to split the vector field in such a way that the solution of (1.11) and evaluations of ρ and \bar{H} are performed only as few times as possible. The *Constant Mean-Field (CMF) method* tries to take this into account, while it can be shown that for smooth data a convergence order of $(\Delta t)^2$ is retained [3]. The smoothness assumption is nontrivial even in the case of MCTDH, and should be regarded even more doubtful in case of MCTDHF.

Nonetheless, according to [2] and [3], the CMF method shows advantageous performance for MCTDH and should certainly be considered as a way to solve the

working equations (2.8) and (2.9) in the context of variational splitting for MCTDHF. Since the system (2.8) is much smaller in dimension in that case than (1.11) for MCTDH because of symmetry, and the step size restrictions associated with $T_{\Delta x}$ are not present in the computations for (2.8), we do not expect to observe an advantage as compared with other methods proposed in Section 2.2.3, however.

2.2.2 The Single Particle Schrödinger Equation

In this section, two different approaches for the solution of the single particle Schrödinger equations (2.7) are discussed. The first results from the space discretization by finite differences currently implemented in the code ([22], [24]). If a pseudospectral space discretization is used, cheap and accurate solution methods using Fast Fourier Transforms (FFTs) are available.

In both cases, we close the system of discrete equations by imposing periodic boundary conditions in space. In the analytical problem an unbounded domain is considered, but for the numerical computations this has to be replaced by a finite regime $[-x_{\text{end}}, x_{\text{end}}]$ and consequently, additional boundary conditions are necessary. The choice of these conditions is arbitrary, but it has to reflect the behavior of the original system and the implementation should be easy. Periodic conditions, where points to the right of the endpoint x_{end} of the finite interval in space are identified with points starting at the left endpoint $-x_{\text{end}}$, satisfy these conditions and moreover yield linear systems with simple structures.

However, we have to be aware that periodic boundary conditions may introduce an undesired solution behavior not related to the physical situation. We may think of a wave that should leave the system and decay for $x \rightarrow \infty$ entering again from the left, to give a crude picture. There are different ways for dealing with this problem. First, we could choose the space grid large enough, so that the wave function has very small amplitude at $x = x_{\text{end}}$ and the effect is negligible. In [2], complex absorbing potentials are suggested. These are also used in [22], [24]. For reasons of simplicity, however, we decided to keep the time integration short enough such that the periodic boundary conditions do not influence the solution behavior.

Space Discretization by Finite Differences

The current implementation of the MCTDHF code ([22], [24]) uses second order finite differences on an equidistant mesh with mesh width Δx to discretize the first and second derivatives in the space variable occurring in the Hamiltonian

from (1.2). That is, we use the approximations

$$\begin{aligned}\psi'(x) &= \frac{\psi(x + \Delta x) - \psi(x - \Delta x)}{2\Delta x} + O((\Delta x)^2), \\ \psi''(x) &= \frac{\psi(x + \Delta x) - 2\psi(x) + \psi(x - \Delta x)}{(\Delta x)^2} + O((\Delta x)^2).\end{aligned}$$

For the time integration of the resulting ODEs derived from (2.7), we use the box scheme. If we denote the Hamiltonian after space discretization by $T_{\Delta x}(t)$, one step with step size Δt of the numerical method is computed from

$$\left(I + \frac{i\Delta t}{2}T_{\Delta x}(t_0 + 1/2\Delta t)\right) \phi_j(t_0 + \Delta t) = \left(I - \frac{i\Delta t}{2}T_{\Delta x}(t_0 + 1/2\Delta t)\right) \phi_j(t_0), \quad (2.10)$$

where $\phi_j(t)$ are the vectors of the single particle functions evaluated at time t and at all spatial mesh points. Since

$$T_{\Delta x}(\hat{t})\phi(x, t) = a\phi(x - \Delta x, t) + b\phi(x, t) + c\phi(x + \Delta x, t), \quad (2.11)$$

where

$$\begin{aligned}a &= -\frac{1}{2(\Delta x)^2} - \frac{i}{2\Delta x}A(\hat{t}), \\ b &= \frac{1}{(\Delta x)^2} + \frac{1}{2}A^2(\hat{t}), \\ c &= -\frac{1}{2(\Delta x)^2} + \frac{i}{2\Delta x}A(\hat{t}),\end{aligned}$$

the system matrix for the system of linear equations (2.10) is *cyclic tridiagonal*, due to the periodic boundary conditions chosen for the space discretization. We adopted an approach for solving such a system efficiently which is given in [18].

Space Discretization by Pseudospectral Methods

Now, we discuss the possible improvements in the computations for (2.7), if instead of finite differences we use pseudospectral methods for space discretization. For descriptions of these methods, see [7], [12] and [20].

The *inverse discrete Fourier transform* of a discrete grid vector (which is assumed to depend on continuous time t) $\hat{U}(t) = (\hat{u}_{-K}(t), \dots, \hat{u}_{K-1}(t))$ is defined as

$$Z(x_l, t) := \text{DFT}^{-1}(\hat{U}) := \sum_{k=-K}^{K-1} \exp\left(\frac{ik\pi x_l}{x_{\text{end}}}\right) \hat{u}_k(t). \quad (2.12)$$

Here, we use an equidistant spatial grid (x_{-K}, \dots, x_K) defined on the interval $[-x_{\text{end}}, x_{\text{end}}]$. Conversely, the *discrete Fourier transform* of $Z(x, t)$ is defined as

$$\hat{u}_k(t) := \text{DFT}(Z) := \frac{1}{2K} \sum_{l=-K}^{K-1} \exp\left(-\frac{ik\pi x_l}{x_{\text{end}}}\right) Z(x_l, t). \quad (2.13)$$

In the pseudospectral method for the solution of the single particle Schrödinger equation (2.7), we make the ansatz

$$\phi(x_l, t) = \text{DFT}^{-1}(\hat{U}) = \sum_{k=-K}^{K-1} \exp\left(\frac{ik\pi x_l}{x_{\text{end}}}\right) \hat{u}_k(t). \quad (2.14)$$

If we substitute this ansatz into collocation equations for (2.7), we obtain an ODE which can be solved efficiently using Strang splitting (see, for example, [9]) and *Fast Fourier Transform* (FFT, introduced in [4]). The algorithm is analogous to [12]:

If we require the ansatz function from (2.14) to satisfy collocation conditions for (2.7) at the grid points x_j , $j = -K, \dots, K-1$, we obtain

$$\begin{aligned} i \frac{d\hat{U}}{dt} &= -\frac{1}{2} D^2 \hat{U} + iA(t) D \hat{U} + \frac{1}{2} A^2(t) \hat{U} + W \hat{U} \\ &=: T \hat{U} + W \hat{U}, \end{aligned} \quad (2.15)$$

where

$$\begin{aligned} D &:= i \cdot \text{diag}\left(\frac{k\pi}{x_{\text{end}}}\right), \quad k = -K, \dots, K-1, \\ W &:= \text{DFT} \circ \text{diag}(U) \circ \text{DFT}^{-1}. \end{aligned}$$

In [12], the situation where the Hamiltonian H is independent of t is considered. In that case, Strang splitting leads to subproblems which can be solved exactly and computed efficiently using FFT:

If H does not depend on t , i. e., $A \equiv 0$ in (1.2), Strang splitting for (2.15) over a time step Δt leads to

$$\hat{U}(t + \Delta t) = \exp\left(-\frac{i}{2}\Delta t W\right) \exp(-i\Delta t T) \exp\left(-\frac{i}{2}\Delta t W\right) \hat{U}(t). \quad (2.16)$$

Thus, the numerical solution is cheap to compute. The second step,

$$\exp(-i\Delta t T), \quad (2.17)$$

is exponentiation of a diagonal matrix, while the first and third steps reduce to

$$\exp\left(-\frac{i}{2}\Delta t W\right) = \text{DFT} \circ \exp\left(\text{diag}\left(-\frac{i}{2}\Delta t U\right)\right) \circ \text{DFT}^{-1}, \quad (2.18)$$

which amounts to the exponentiation of a diagonal matrix and one application of FFT and FFT^{-1} , respectively.

In our case, where T explicitly depends on time t (due to the given laser pulse $A(t)$), we have to use a numerical approximation to (2.17). Since the matrix exponentials involve only diagonal matrices, the problems are equivalent to solving sets of scalar, non-autonomous, homogeneous linear ODEs

$$y'(t) = a(t)y(t). \quad (2.19)$$

Since in the scalar case, $a(t)$ and $\int a(t)$ commute, the solution of (2.19) is

$$y(t) = \exp\left(\int_{t_0}^t a(\tau) d\tau\right) y(t_0). \quad (2.20)$$

For the purpose of the numerical solution, we can use any suitable quadrature formula to approximate $\int_{t_0}^t a(\tau) d\tau$ in (2.20).

To use this idea for the solution of (2.15), we choose a simple second order quadrature formula to approximate (2.20),

$$\int_t^{t+\Delta t} a(\tau) d\tau \approx \Delta t a\left(t + \frac{1}{2}\Delta t\right).$$

We should keep in mind that we could just as well replace this by higher order quadrature formulae, but our choice seems natural, since Strang splitting (2.16) introduces a second order approximation anyway.

The resulting procedure is the exponential midpoint rule applied in each sub-step of Strang splitting, see [14]. Consequently, instead of (2.16) we have to compute

$$\begin{aligned} \hat{U}(t + \Delta t) &= \exp\left(-\frac{i}{2}\Delta t W\right) \cdot \\ &\quad \cdot \exp\left(\Delta t \left(\frac{i}{2}D^2 + A(t + 1/2\Delta t)D - \frac{i}{2}A^2(t + 1/2\Delta t)\right)\right) \cdot \\ &\quad \cdot \exp\left(-\frac{i}{2}\Delta t W\right) \hat{U}(t). \end{aligned} \quad (2.21)$$

The computational tasks are equivalent to those for the computation of (2.16).

2.2.3 The Reduced Working Equations

To solve the reduced working equations (2.8) and (2.9), where the Hamiltonian is reduced to the particle-particle potential V , several approaches are worth trying. First, we discuss [16, (5.1)] and its dual version, [16, (5.2)]. Both versions rely on a splitting of the vector field into the parts associated with (2.8) and (2.9).

One step with time step Δt starting at a point $t = t_0$ of the first algorithm reads

$$\phi(t_0 + 1/2\Delta t) = \phi(t_0) - \frac{i}{2}\Delta t B_V(a(t_0), \phi(t_0))\phi(t_0), \quad (2.22)$$

$$a(t_0 + \Delta t) = \exp(-i\Delta t A_V(\phi(t_0 + 1/2\Delta t)))a(t_0), \quad (2.23)$$

$$\begin{aligned} \phi(t_0 + \Delta t) = \phi(t_0 + 1/2\Delta t) - \\ - \frac{i}{2}\Delta t B_V(a(t_0 + \Delta t), \phi(t_0 + \Delta t))\phi(t_0 + \Delta t). \end{aligned} \quad (2.24)$$

This splitting method consists of one half-step of the explicit Euler method (2.22), which is straightforward to compute, one step of the exponential midpoint rule (2.23), which can be computed cheaply using for example Lanczos' method¹ (cf. [14]), and finally a half-step of the implicit Euler method (2.24). This implicit step can be solved by fixed point iteration, where the starting guess is simply a linear extrapolation of the values of ϕ at $t = t_0$ and $t = t_0 + 1/2\Delta t$, see [16]. Note that the last step is the adjoint method of the scheme used in (2.22). For a general discussion of splitting methods of this type, see [9].

The orthogonality relation (1.10) is not preserved by this integration scheme, see [16]. Consequently, (1.10) has to be enforced eventually. This could, for example, be done in every step by using the Gram-Schmidt method as in [22], [24]. We propose to use a projection method from [9], see 2.2.3.

The dual version of the last algorithm preserves orthogonality, however, see [16]. Thus, alternatively we can use the method defined by

$$a(t_0 + 1/2\Delta t) = \exp\left(-\frac{i}{2}\Delta t A_V(\phi(t_0))\right) a(t_0), \quad (2.25)$$

$$\phi(t_0 + \Delta t) = \phi(t_0) - i\Delta t B_V(a(t_0 + 1/2\Delta t), \phi^{1/2})\phi^{1/2}, \quad (2.26)$$

$$a(t_0 + \Delta t) = \exp\left(-\frac{i}{2}\Delta t A_V(\phi(t_0 + \Delta t))\right) a(t_0 + 1/2\Delta t), \quad (2.27)$$

where $\phi^{1/2} := 1/2(\phi(t_0) + \phi(t_0 + \Delta t))$. (1.10) is preserved by this integration method if the implicit step (2.26) is solved accurately enough. This is even true if in the fixed point iteration, we evaluate ρ and \bar{H} in (2.26) at $a(t_0 + 1/2\Delta t)$ and $\phi(t_0) - \frac{i}{2}\Delta t B_V(a(t_0), \phi(t_0))\phi(t_0)$ and freeze ρ and \bar{H} , but update the projection P [16].

Evaluation of Integrals

To evaluate the right-hand sides of the working equations (2.8) and (2.9), we have to compute the density matrix ρ as defined in (1.16), the meanfield operator

¹Actually, we use a Fortran module described in [19]. There, a Padé approximation method is used for dense matrices as in our case, and Lanczos' method only for sparse matrices.

matrix \bar{H} from (1.17), the projector P and the Galerkin matrix $A_V(\phi)$ according to (1.13). The computation of all these quantities apart from ρ requires numerical quadrature. For the evaluation of $A_V(\phi)$, an integral over all f degrees of freedom has to be approximated, the computations of ρ and \bar{H} involve integrals in $f - 1$ dimensions, and the projector P is a sum of integrals in one space dimension, respectively.

Due to the orthogonality relation (1.10), the computation of ρ is reduced to

$$\rho_{jl} = \sum_{j_2=1}^N \cdots \sum_{j_f=1}^N \bar{a}_{jj_2 \dots j_f} a_{lj_2 \dots j_f}. \quad (2.28)$$

Since V describes the relations between any two particles and (1.10) holds, the integrals occurring in the computations of \bar{H} and A_V are reduced to a sum of integrals in two dimensions. This may still be an intractable computation, however. Consequently, V may be expressed as

$$V(x, y) = \sum_{i=1}^D \lambda_i v_i(x) v_i(y).$$

Some methods to derive such an expansion are described in [2], the method used in [22], [24] is related to these ideas. Using this approach, the integrals are reduced to sums of products of integrals in one space dimension.

Since the choice of nodes used in the numerical quadrature is given from the space discretization, simple first order quadrature using the (available) equidistant grid points is used. Namely, the integrals are approximated by simple (unweighted) summation. From [22], [24] it seems that this does not result in critical inaccuracy. This point needs to be kept in mind, however.

Finally, we would like to mention a simplification from [22], [24]. For the purpose of speeding up the calculations, the quadratures associated with the particle-particle potential V are calculated with less accuracy (where fewer abscissae are used) in regions where this seems justified from the application's point of view. We do not give any details here.

Singular Density Matrix

In both implementations [22], [24] and [2], it is assumed that the representations (1.12) and (1.14) are equivalent. Unfortunately, however, it is possible that the leading matrix ρ in (1.14) becomes singular. In that case, we cannot use (1.12). In both implementations, the density matrix has been modified to enforce regularity.

In [2], ρ is replaced by

$$\rho_{\text{reg}} := \rho + \varepsilon \exp(-\rho/\varepsilon),$$

where ε is a small number, usually between 10^{-8} and 10^{-14} , depending on the chosen accuracy of the numerical integration scheme.

In [22], [24], a small quantity EPS is added to the diagonal of ρ , where usually $\text{EPS} = 10^{-12}$. This is done indiscriminately of the fact whether ρ is singular or nonsingular in that step. Apparently, this modification is not critical.

In the remainder of this section, we discuss the case of singular ρ with more mathematical rigor. To this end, we formulate the problem of the solution of (1.14) in a more abstract setting.

Consider the autonomous ODE

$$\dot{y} = f(y)$$

on a manifold \mathcal{M} . This can be expressed as $y = \chi(z)$, where in our case the parameter space is $z = (a, \phi)$ and the manifold \mathcal{M} is given by the ansatz (1.6). The solution of the ODE on the manifold is defined as the least squares problem

$$\|\dot{y} - f(y)\|_2 \rightarrow \min \iff \quad (2.29)$$

$$\|X\dot{z} - f(\chi(z))\|_2 \rightarrow \min, \quad (2.30)$$

where $X(z) := \chi'(z)$. The least squares problem (2.30) can in principle be solved by the solution of the *normal equations*

$$X^* X \dot{z} = X^* f(\chi(z)), \quad (2.31)$$

where $X^* := \bar{X}^T$ is the hermite transpose of the matrix X . The conditioning of these equations with respect to perturbations in f depends on the form of the perturbation. If the right-hand side of a perturbed version of (2.31) is of the form $X^*(f(\chi(z)) + \delta)$, the problem is well-conditioned, whereas we are faced with an ill-conditioned problem if the right-hand side is of the more general form $X^* f(\chi(z)) + \delta$.

In our case, (1.14) is a part of (2.31) and ρ is a submatrix of the mass matrix $X^* X$. The way the data for (1.14) is computed in [22], [24] suggests that we are faced with the favorable situation where the right-hand side is of the form $X^*(f(\chi(z)) + \delta)$. Since the right-hand side lies in the image of ρ , no ill-conditioning results. However, it may be desirable to replace the regularization strategy from [22], [24] with mathematically more sound methods. One possible implementation could be to transform (1.14) so that the leading matrix is equal to the singular value decomposition of ρ . Equations corresponding to the singular values smaller than a certain tolerance could be ignored in the computations.

Reorthogonalization

In the original program version [22], [24], reorthogonalization is performed after every step of the Runge-Kutta method using the Gram-Schmidt method. Alternatively, we intend to use a reorthogonalization suggested in [9]. To this end, we

compute the singular value decomposition of the solution matrix $Y = [\phi_1, \dots, \phi_N]$ (where the columns contain the values of the ϕ_j at the points of the spatial grid),

$$Y = U^T \Sigma V. \quad (2.32)$$

In the last equation, U^T is a $2K \times N$ matrix ($2K$ being the number of spatial gridpoints), V an $N \times N$ matrix, both having orthonormal columns, and $\Sigma = \text{diag}(\sigma_1, \dots, \sigma_N)$ contains the singular values. Since orthogonality is violated only from numerical errors, $\sigma_j \approx 1$, and we can use the orthogonal matrix

$$\tilde{Y} := U^T V \quad (2.33)$$

as the numerical approximation which satisfies (1.10). This projection method associated with the so-called *Stiefel manifold* is discussed in more detail in [9]. This straight-forward method of enforcing orthogonality seems more appropriate for our task than Lie-group methods or other more sophisticated geometric integration methods also described in [9].

2.3 Error Estimation

In [22], [24], numerical errors in the time propagation are estimated using mesh halving. In this approach, the numerical solution of order p is computed on a grid with step size Δt and this approximation is denoted by z_Δ . Subsequently, we choose a second mesh with step size $\Delta t/2$. On this mesh, we compute the numerical solution based on the same numerical method to obtain the approximation $z_{\Delta/2}$. Using these two quantities, we define

$$\mathcal{E}(\tau) := \frac{1}{1 - 2^p} (z_{\Delta/2}(\tau) - z_\Delta(\tau)) \quad (2.34)$$

as an error estimate for the approximation $z_{\Delta/2}$ at all points τ in the grid with mesh width Δ . Assume that the global error $\delta(\tau) = z(\tau) - p_{\Delta/2}(\tau)$ of the numerical solution at every grid point τ can be expressed in terms of the principal error function $e(\tau)$,

$$\delta(\tau) = e(\tau) \Delta t^p + O(\Delta t^{p+1}), \quad (2.35)$$

where $e(\tau)$ is independent of Δt . Then obviously the quantity $\mathcal{E}(\tau)$ satisfies $\mathcal{E}(\tau) - \delta(\tau) = O(\Delta t^{p+1})$ at all the points τ of the coarser grid with mesh width Δt .

Alternatively, we consider error estimates based on *Defect Correction*, see [10] and [11]. These provide asymptotically correct error estimates for smooth problems without expensive computations on grids with step size $\Delta t/2$. Rather, in addition to the computation of the basic solution z_Δ , a neighboring problem is solved on the same grid. Unfortunately, however, currently no version of defect correction

is available which can cope with unsmooth problems resulting from space semi-discretization of the Schrödinger equation. A complete documentation of these observations can be found in [10] and [11]. Further work will be devoted to this subject.

2.4 Step Size Control

To test our algorithms, we first computed our test runs on uniform time grids, where for the purpose of comparison, we disabled step size control in the original code [22], [24]. This still yields valuable insights, since it turned out that the step size variation in the original code is quite moderate². Figures 2.1 and 2.2 show the step sizes produced in a test run of the original code where step size control was enabled, plotted against the number of the respective step in the time integration. The plot from Figure 2.1 was computed for a single particle model where $N = f = 1$, while Figure 2.2 shows the results for $N = f = 2$ (these equations are explicitly stated in Section 1.2). Overall, the variation in the step sizes is very small, not larger than a factor of two globally.

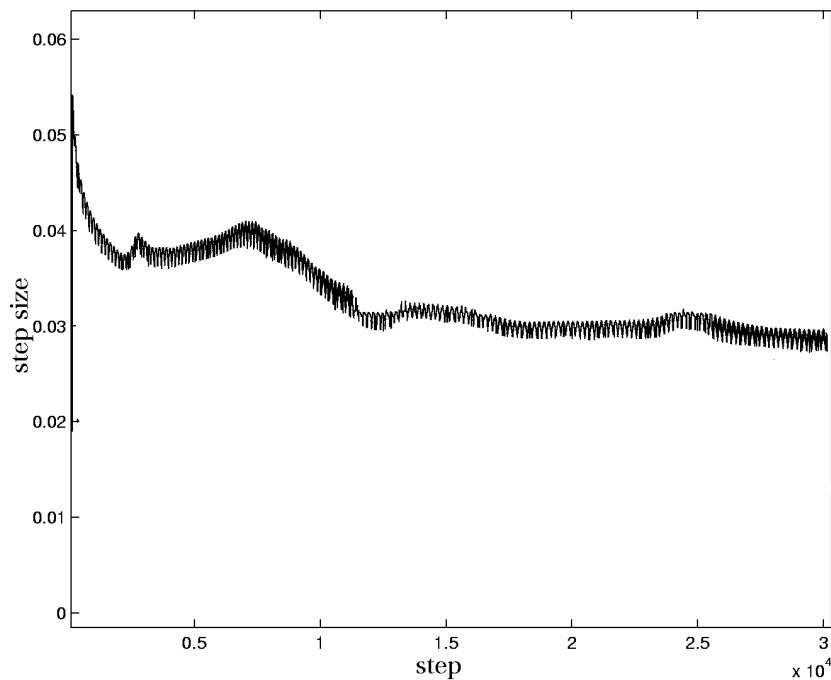


Figure 2.1: Step sizes for the single particle case

²This behavior depends on the smoothness of the initial values, which influences the time evolution of the solution critically, however.

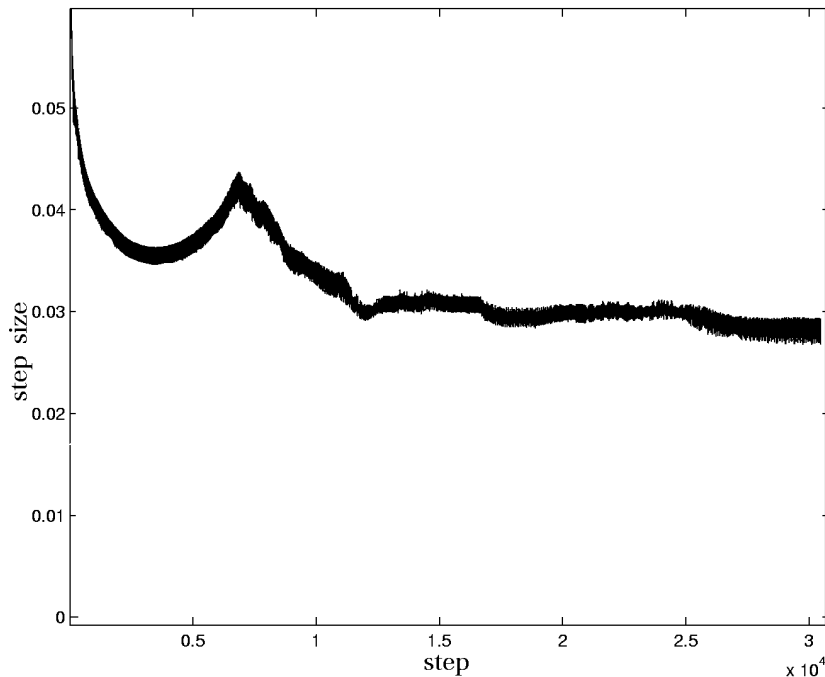


Figure 2.2: Step sizes for the example from Section 1.2

2.5 Discussion

Obviously, the potential for improving the efficiency of the computations in the MCTDHF method is vast.

Firstly, it is possible that alternative approximations for the solution of (1.1) are found to work satisfactorily, which reduce the computational complexity significantly as compared to MCTDHF. Moreover, we have to be aware of the limitations the MCTDHF approach suffers from. On the one hand, we approximate the exact wave function ψ^* on a manifold \mathcal{M} . This error can be reduced arbitrarily if a sufficient number of configurations is used in the ansatz (1.6), however, cf. [2]. Moreover, the Dirac-Frenkel variational principle (1.7) does not yield the best approximation of ψ^* on the manifold \mathcal{M} , but uses a linearization and subsequent projection to \mathcal{M} . The error introduced in this approximation step is analyzed in [15]. For a smooth particle-particle potential (1.4), the error of the solution ψ computed by the MCTDHF method on a compact interval, as compared with the exact wave function ψ^* satisfies

$$\|\psi - \psi^*\| \leq d(t) + Ce^{Kt} \int_0^t d(s) ds, \quad (2.36)$$

where $d(t) := \text{dist}(\psi(t), \mathcal{M})$, $K := 2\kappa\delta$, and $C := \beta + \kappa(\beta + 3\mu)$. Here, κ denotes the curvature of the manifold \mathcal{M} , and β , δ and μ are problem-specific constants

giving bounds for the particle-particle potential V , the Hamiltonian H and the distance of iH applied to both ψ and ψ^* from the tangent space of \mathcal{M} . For a more detailed description, see [15]. Note that this estimate constitutes only an upper bound and might be rather pessimistic. In the case where the curvature κ is small, long term integration of the MCTDHF equations is likely to yield useful results.

In the case of unsmooth potentials, however, the analogous estimates are less promising, see [15]. This is only relevant in practice for the Coulomb potential in three space dimensions. This case is not considered in this report, where we focus on problems in one space dimension.

Big potential gain in the efficiency of numerical computations can be expected from choosing an optimal space discretization. In Section 2.2.2 we expressed our confidence that using pseudospectral methods instead of simple finite differences will reduce the computational complexity significantly. In higher dimensions, even more speed-up should be possible by choosing a suitable space discretization. Adaptive spatial grids or moving meshes might also be considered.

Our first goal, however, is to improve the performance of time integration. In Section 2.1 we discussed methods which we expect to show a more favorable behavior than explicit Runge-Kutta methods implemented in [22], [24].

To conclude, in Figure 2.3 we give a graphical representation of the time composition of the most important components of the whole algorithm, as it is implemented in [22], [24].

The largest part is constituted by the computation of the data for (1.14), which takes up 72% of the overall runtime. Particularly the calculation of the density matrix ρ and the mean-field operator matrix \bar{H} are time consuming, see (1.16) and (1.17). The second largest part consists of the computation of the Galerkin matrix (1.13) which amounts to 12% of the computation time. The solution of the Runge-Kutta equations, and the other parts of the computation, like reorthogonalization etc., do not contribute significantly to the computation time. Both factors take up 8% of the computational effort. Consequently, we expect the biggest potential gain in the speed-up of the summations and quadratures necessary to compute the problem data for the working equations. However, the same goal can be achieved if numerical integration methods for the ODEs are employed which do not suffer from step size restrictions for stability and accuracy, or by using a good mesh selection strategy. Moreover, freezing strategies [2] should be tried. Both measures imply that the problem data have to be evaluated less frequently, reducing the computational effort significantly.

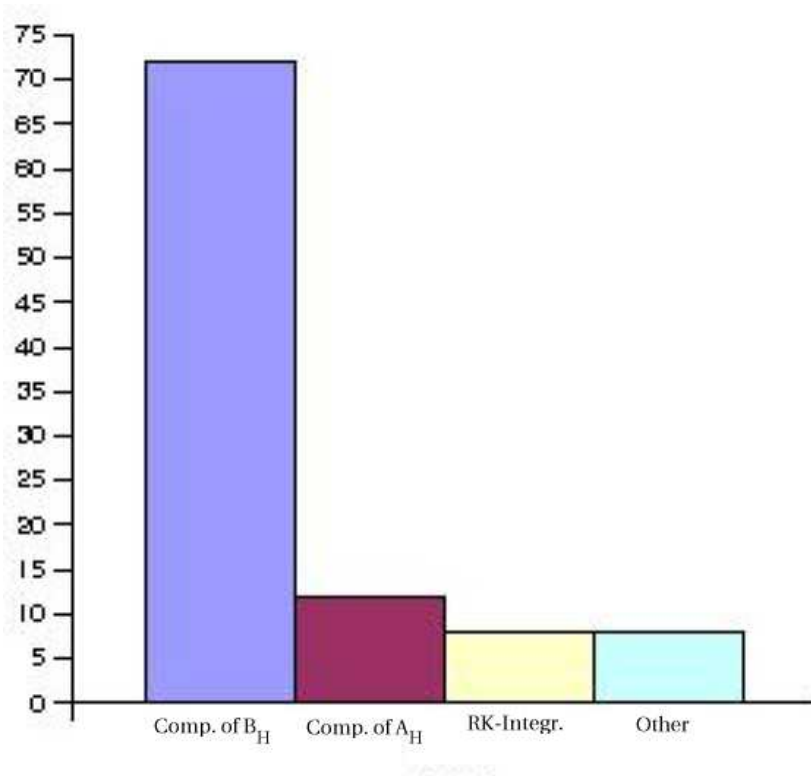


Figure 2.3: Time composition of MCTDHF computations.

Summary and Outlook

In this report, we discussed various approaches applicable for the numerical solution of the systems of nonlinear Schrödinger equations which result from the multi-configuration time-dependent Hartree-Fock (MCTDHF) method for the approximate integration of the time-dependent Schrödinger equation arising in ultrafast laser dynamics. Our goal is to implement alternative space discretization schemes and time integration methods to enhance the efficiency of an available code for the solution of the working equations resulting from a variational principle applied to compute the quantities associated with our nonlinear ansatz for the approximate computation of the wave function. We hope to increase the class of computationally tractable problems and widen the range of applicability of the MCTDHF method.

References

- [1] A. Bandrauk, A. Chelkowski: *On laser Coulomb explosion imaging of proton motion*. Chem. Phys. Letters 336 (2001), pp. 518–522.
- [2] M.H. Beck, A. Jäckle, G.A. Worth, H.D. Meyer: *The multiconfiguration time-dependent Hartree (MCTDH) method: A highly efficient algorithm for propagating wavepackets*. Phys. Rep. 324 (2000), pp. 1–105.
- [3] M.H. Beck, H.D. Meyer: *An efficient and robust integration scheme for the equations of the multiconfiguration time-dependent Hartree (MCTDH) method*. Z. Phys. D 42 (1997), pp. 113–129.
- [4] J. Cooley, J. Tukey: *An Algorithm for the Machine Calculation of Complex Fourier Series*. Math. Comp. 19 (1965), pp. 297–301.
- [5] P.A.M. Dirac: *Note on Exchange Phenomena in the Thomas Atom*. Proc. Cambridge Phil. Soc. 26 (1939), pp. 376–385.
- [6] C. Fabian: *Dynamik von Multielektronensystemen unter dem Einfluss hochintensiver Laserfelder*. Ph. D. Thesis, Institut für Photonik, Vienna Univ. of Technology, Austria, 2003.
- [7] B. Fornberg: *A Practical Guide to Pseudospectral Methods*. Cambridge University Press, Cambridge, 1996.
- [8] J. Frenkel: *Wave Mechanics, Advanced General Theory*. Clarendon Press, Oxford, 1934.
- [9] E. Hairer, C. Lubich, G. Wanner: *Geometric Numerical Integration*. Springer-Verlag, Berlin-Heidelberg-New York, 2002.
- [10] H. Hofstätter, O. Koch: *Splitting Defect Correction*. AU-RORA TR-2003-23, Inst. for Appl. Math. and Numer. Anal., Vienna Univ. of Technology, Austria, 2003. Available at <http://www.math.tuwien.ac.at/~aurora/Aurora/start.html>.
- [11] H. Hofstätter, O. Koch: *Defect Correction for Geometric Integrators*. In *Proceedings of APLIMAT*.
- [12] T. Jahnke, C. Lubich: *Error bounds for exponential operator splittings*. BIT 40 (2000), pp. 735–744.
- [13] F. Krausz, T. Brabec: *Intense few-cycle laser fields: frontiers of nonlinear optics*. Rev. Mod. Phys. 72 (2000), pp. 545–562.

- [14] C. Lubich: *Integrators for Quantum Dynamics: A Numerical Analyst's Brief Review*. In *Quantum Simulations of Complex Many-Body Systems: From Theory to Algorithms, Lecture Notes* (J. Grotendorst, D. Marx, A. Muramatsu, eds.), John von Neumann Institute for Computing, Vol. 10 of *NIC Series*, 2002, pp. 459–466.
- [15] C. Lubich: *On Variational Approximations in Quantum Molecular Dynamics*. Submitted to *Math. Comp.*
- [16] C. Lubich: *A Variational Splitting Integrator for Quantum Molecular Dynamics*. To appear in *Appl. Num. Math.*
- [17] J. S. Parker, L. R. Moore, K. T. Taylor: *Accurate computational methods for two-electron atom-laser interactions*. *Optics-Express* 8 (2001), pp. 436–441.
- [18] W. Press, B. Flannery, S. Teukolsky, W. Vetterling: *Numerical Recipes in FORTRAN77*, 2nd edn. Cambridge University Press, Cambridge, 1993.
- [19] R. Sidje: *Expokit: A Software Package for Computing Matrix Exponentials*. *ACM Trans. Math. Softw.* 24 (1998)(1), pp. 130–156.
- [20] L. Trefethen: *Spectral Methods in MATLAB*. SIAM, Philadelphia, 2000.
- [21] V. Veniard, R. Taieb, A. Maquet: *Photoionization of Atoms Using Time-Dependent Density Functional Theory*. *Laser Physics* 13 (2003), pp. 465–474.
- [22] J. Zanghellini, M. Kitzler, T. Brabec, A. Scrinzi: *Testing the Multi-Configuration Time-Dependent Hartree-Fock Method*. To appear in *J. Phys. B: At. Mol. Phys.*
- [23] J. Zanghellini, M. Kitzler, C. Fabian, T. Brabec, A. Scrinzi: *Multi-electron dynamics in strong laser fields*. To appear.
- [24] J. Zanghellini, M. Kitzler, C. Fabian, T. Brabec, A. Scrinzi: *An MCT-DHF approach to multi-electron dynamics in laser fields*. *Laser Physics* 13 (2003)(8), pp. 1064–1068.